

RL-TR-96-144
Final Technical Report
July 1996



HOLOGRAPHIC RANDOM ACCESS MEMORIES

Northrop Grumman

Susan Raffensperger

19970211 018


APPROVED FOR PUBLIC RELEASE; DISTRIBUTION UNLIMITED.

Rome Laboratory
Air Force Materiel Command
Rome, New York

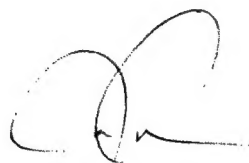
DTIC QUALITY INSPECTED 3

This report has been reviewed by the Rome Laboratory Public Affairs Office (PA) and is releasable to the National Technical Information Service (NTIS). At NTIS, it will be releasable to the general public, including foreign nations.

RL-TR-96-144 has been reviewed and is approved for publication.

APPROVED: 
BERNARD J. CLARKE, Captain, USAF
Project Engineer

FOR THE COMMANDER:



JOSEPH CAMERA
Technical Director
Intelligence & Reconnaissance Directorate

If your address has changed or if you wish to be removed from the Rome Laboratory mailing list, or if the addressee is no longer employed by your organization, please notify Rome Laboratory/ (IRAP), Rome NY 13441. This will assist us in maintaining a current mailing list.

Do not return copies of this report unless contractual obligations or notices on a specific document require that it be returned.

REPORT DOCUMENTATION PAGE

Form Approved
OMB No. 0704-0188

Public reporting burden for this collection of information is estimated to average 1 hour per response, including the time for reviewing instructions, searching existing data sources, gathering and maintaining the data needed, and completing and reviewing the collection of information. Send comments regarding this burden estimate or any other aspect of this collection of information, including suggestions for reducing this burden, to Washington Headquarters Services, Directorate for Information Operations and Reports, 1215 Jefferson Davis Highway, Suite 1204, Arlington, VA 22202-4302, and to the Office of Management and Budget, Paperwork Reduction Project (0704-0188), Washington, DC 20503.

1. AGENCY USE ONLY (Leave Blank)		2. REPORT DATE July 1996		3. REPORT TYPE AND DATES COVERED Final Nov 92 - Dec 95	
4. TITLE AND SUBTITLE HOLOGRAPHIC RANDOM ACCESS MEMORIES				5. FUNDING NUMBERS C - F30602-92-C-0073 PE - 62702F PR - 4594 TA - 15 WU - J5	
6. AUTHOR(S) Susan Raffensperger					
7. PERFORMING ORGANIZATION NAME(S) AND ADDRESS(ES) Northrop Grumman Electronics & Systems Integration Division 2301 W 120th Street Hawthorne CA 90251-5023				8. PERFORMING ORGANIZATION REPORT NUMBER N/A	
9. SPONSORING/MONITORING AGENCY NAME(S) AND ADDRESS(ES) Rome Laboratory/IRAP 32 Hangar Rd Rome NY 13441-4114				10. SPONSORING/MONITORING AGENCY REPORT NUMBER RL-TR-96-144	
11. SUPPLEMENTARY NOTES Rome Laboratory Project Engineer: Bernard J. Clarke, Captain, USAF/IRAP/ (315) 330-4581					
12a. DISTRIBUTION/AVAILABILITY STATEMENT Approved for public release; distribution unlimited.				12b. DISTRIBUTION CODE	
13. ABSTRACT (Maximum 200 words) This program, originally proposed in early 1991 and eventually funded in late 1992, represented a pioneering effort to demonstrate, using only commercially available components and proven technologies, the technical feasibility of 3-D holographic memories. Building on work done at Northrop, which indicated that relatively high data storage densities (gigabit/cubic cm) could be achieved in iron-doped lithium niobate and on novel architectural concepts developed jointly by Northrop and California Institute of Technology, the objectives of this program were to show that: 1) by using a combination of spatial and angle multiplexing techniques, storage terabits could eventually be achieved within 100 cubic cm iron-doped lithium niobate; 2) random access times of less than 10 microsec could be achieved by using non-mechanical (acousto-optic) reference beam scanning techniques; and 3) adequate, if not optimal, SLMs and CCD arrays were not available. The above objectives were to be achieved using a WORM (write once/read many times) memory architecture that circumvented, to the greatest extent possible, the recognized read/write sensitivity limitations of iron-doped lithium niobate.					
14. SUBJECT TERMS Holographic, Optical memories, Lithium niobate, Mass data storage				15. NUMBER OF PAGES 24	
				16. PRICE CODE	
17. SECURITY CLASSIFICATION OF REPORT UNCLASSIFIED	18. SECURITY CLASSIFICATION OF THIS PAGE UNCLASSIFIED	19. SECURITY CLASSIFICATION OF ABSTRACT UNCLASSIFIED	20. LIMITATION OF ABSTRACT UL		

TABLE OF CONTENTS

1.0	Introduction	2
2.0	Architecture	4
3.0	Results	10
4.0	Conclusions	14
	References	15

DTIC QUALITY INSPECTED 3

1.0 Introduction

The traditional advantages of 3-D holographic memories are high storage density and parallel access capability. These features were recognized in the early 1960's [1, 2, 3, 4] and serious efforts toward the practical implementation of such memories were undertaken. Unfortunately, owing to a lack of suitable data input and output transducers, efficient, reliable lasers, and, to some extent, appropriate storage media, these early efforts failed. The recent emergence of fast, efficient, megapixel spatial light modulators (SLMs) and CCD arrays, combined with a rapid maturing of solid-state, blue-green laser technology and an improved understanding of storage media physics has, however, caused a resurgence of interest in holographic memories.

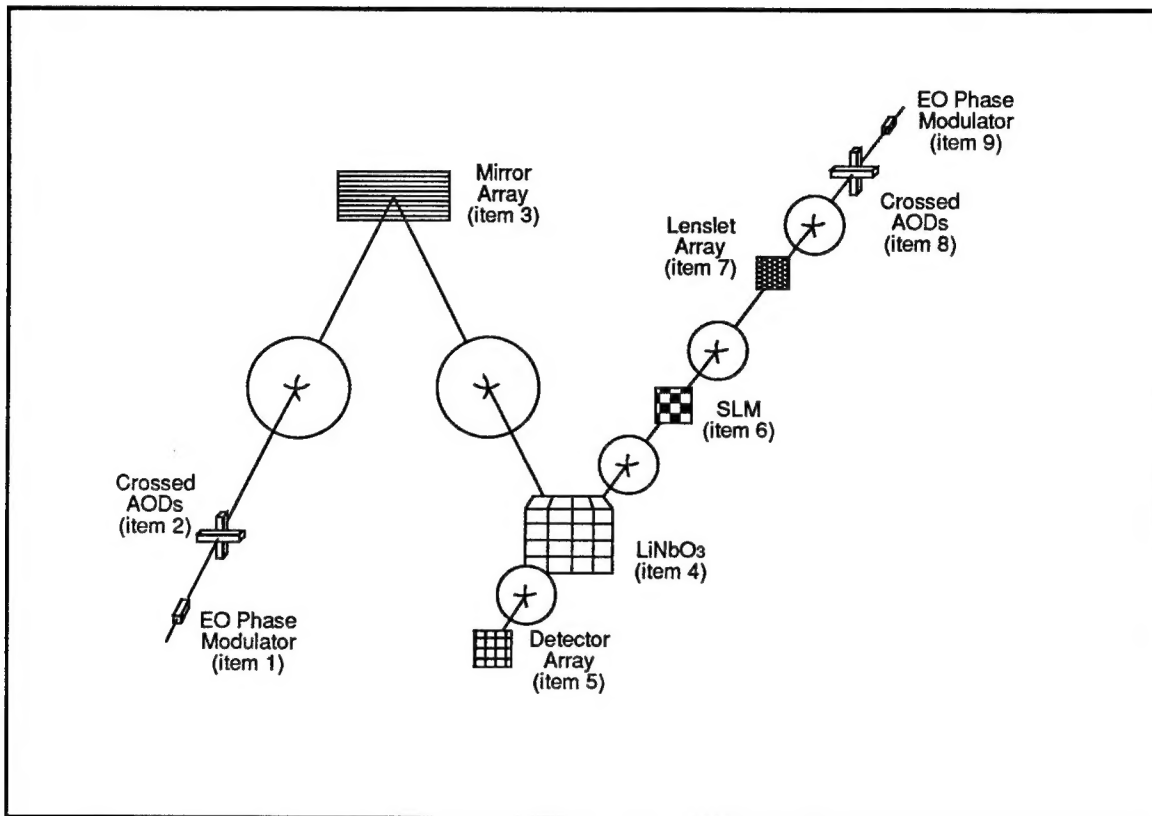


Figure 1: Originally proposed memory architecture.

This program, originally proposed in early 1991 and eventually funded in late 1992, represented a pioneering effort to demonstrate, using only commercially available components and proven technologies, the technical feasibility of 3-D holographic memories. Building on work done at Northrop, which indicated that relatively high data storage densities ($>10^9$ bits/cm³) could be achieved in iron-doped lithium niobate (Fe:LiNbO₃) [5,6], and on novel architectural concepts developed jointly by Northrop and California Institute of Technology, the objectives of this program were to show that:

- (1) by using a combination of spatial and angle multiplexing techniques, storage capacities of 10^{12} bits could eventually be achieved within 100 cm³ of Fe:LiNbO₃;

(2) random access times of less than 10 μsec could be achieved by using non-mechanical (acousto-optic) reference beam scanning techniques; and

(3) adequate, if not optimal, SLMs and CCD arrays were now available.

The above objectives were to be achieved using a WORM (write once/read many times) memory architecture that circumvented, to the greatest extent possible, the recognized read/write sensitivity limitations of Fe:LiNbO₃.

Figure 1 shows the architecture originally proposed. To achieve both spatial as well as angle multiplexing, a novel mirror array (item 3) was designed to direct the reference beam to different spatial locations within the Fe:LiNbO₃ storage medium (item 4), while still permitting the reference beam to be scanned linearly in order to achieve angle multiplexing at each spatial location. Access to different elements of the mirror array was to be achieved by scanning the reference beam in a direction orthogonal to the direction used for multiplexing. Reference beam scanning in both directions was to be achieved using (non-mechanical) acousto-optic beam deflectors (item 2). The data (object) beam was to be directed to each storage location using two additional acousto-optic scanners (item 8), combined with very fast Fourier transformation optics.

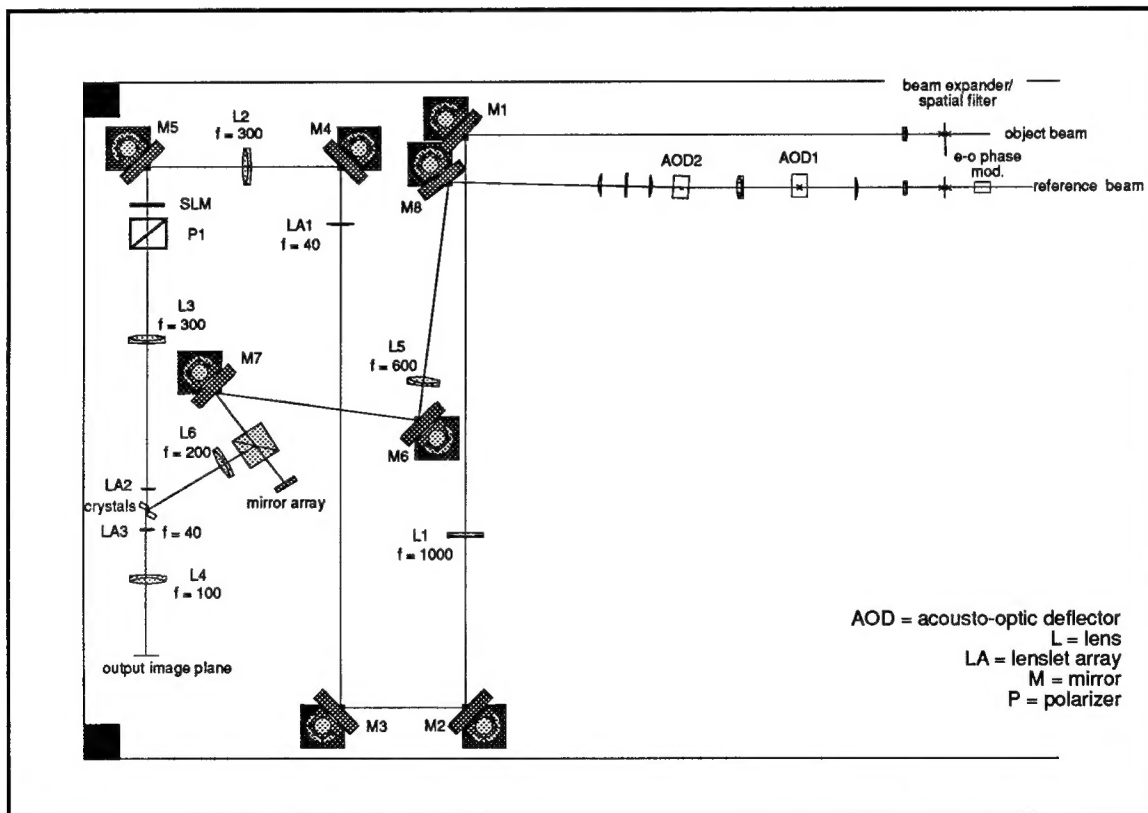


Figure 2: HRAM optical layout.

As discussed in the Architecture section that follows, the actual memory breadboard differed in two (non-essential) ways from that shown in Figure 1: (1) because only two functional acousto-optic scanners were available, the object beam was scanned

mechanically; and, (2) because a rectilinear diffuser (phase-encoder) with a pitch equal to that of the SLM was not immediately available, image-space (instead of Fourier-space) holograms were stored within the Fe:LiNbO₃.

California Institute of Technology was also let a \$50,000 technical services subcontract to support this effort. The results of their activities are summarized in the Appendix.

2.0 Architecture

2.1 Overview. Figure 2 shows a plan view of the HRAM architecture. Key components of the system included two acousto-optic Bragg cells (Crystal Technology model 4080-2) for reference beam scanning, an electro-optic phase modulator (New Focus model 4002) to compensate for frequency shifts introduced by the Bragg cells, a faceted mirror array for directing the reference beam to different locations within the storage medium, lenslet arrays to form and direct data images to each storage location, a twisted nematic liquid crystal SLM (from an Epson video projector, model E1020, 320 x 220) that served as the data input transducer and a CCD camera (Cohu model 4815-5000/0000) that served as the data output transducer. The light source was a Coherent Innova 300, 1 Watt, CW, argon-ion laser tuned for 488 nm output.

2.2 Storage Medium. The storage medium consisted of four [1 x 1.5 x 2 cm], z-cut, 0.015 mole-percent iron-doped lithium niobate crystals (Fe:LiNbO₃). Holograms were stored in four locations within each crystal, with all 16 locations arranged in a regular 4 by 4 grid. Figure 3 illustrates how the crystals were configured relative to the object (data) and reference beams. The crystal axes were oriented within the plane of incidence, with the object and reference beams each nominally incident on the crystals at 30° to the crystal normals. The total included angle between each object and reference beam pair was approximately 60° in air. The reference beam incidence angle was scanned to provide angular multiplexing at each storage location. The polarization used was extraordinary, i.e., the polarization of both beams was within the plane of incidence.

2.3 The Mirror Array. The faceted mirror array, a novel feature of the HRAM design, is shown in greater detail in Figure 4. The array was made up of four distinct segments, each segment having four facets. The segments were stacked at incremented angles to provide horizontal spatial multiplexing, i.e., to direct the reference beam to the appropriate column of the 4 by 4 grid of storage locations. The angle of each facet provided vertical spatial multiplexing. The beam was directed to one of the 16 storage locations by the reference beam scan generator, which selected the appropriate mirror facet.

As shown in Figure 5, the same technique used for making blazed gratings was employed to fabricate the mirror array. This technique involved using a diamond tip to cut grooves on the substrate. The angles of the grooves were accurately controlled by the tilt of the diamond tip with respect to the substrates. The width of each groove was controlled by the number of cuts in the same groove. The mirror was manufactured by Diffraction Products in Woodstock, Illinois.

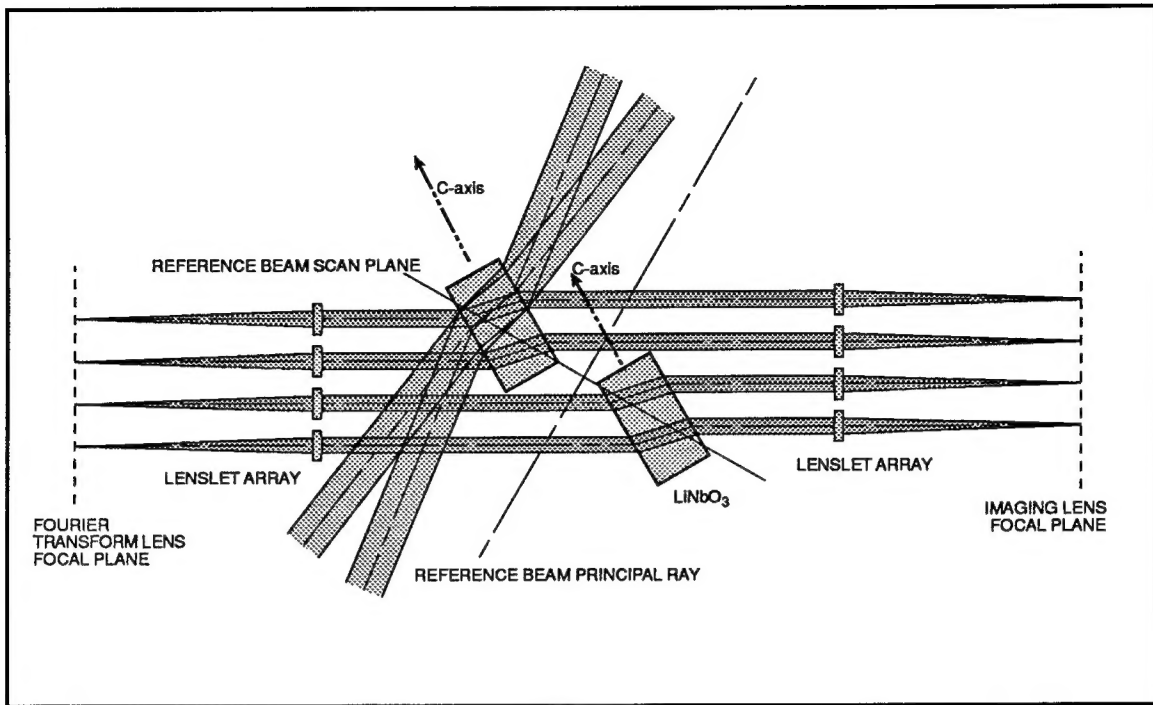


Figure 3: Spatial multiplexing detail.

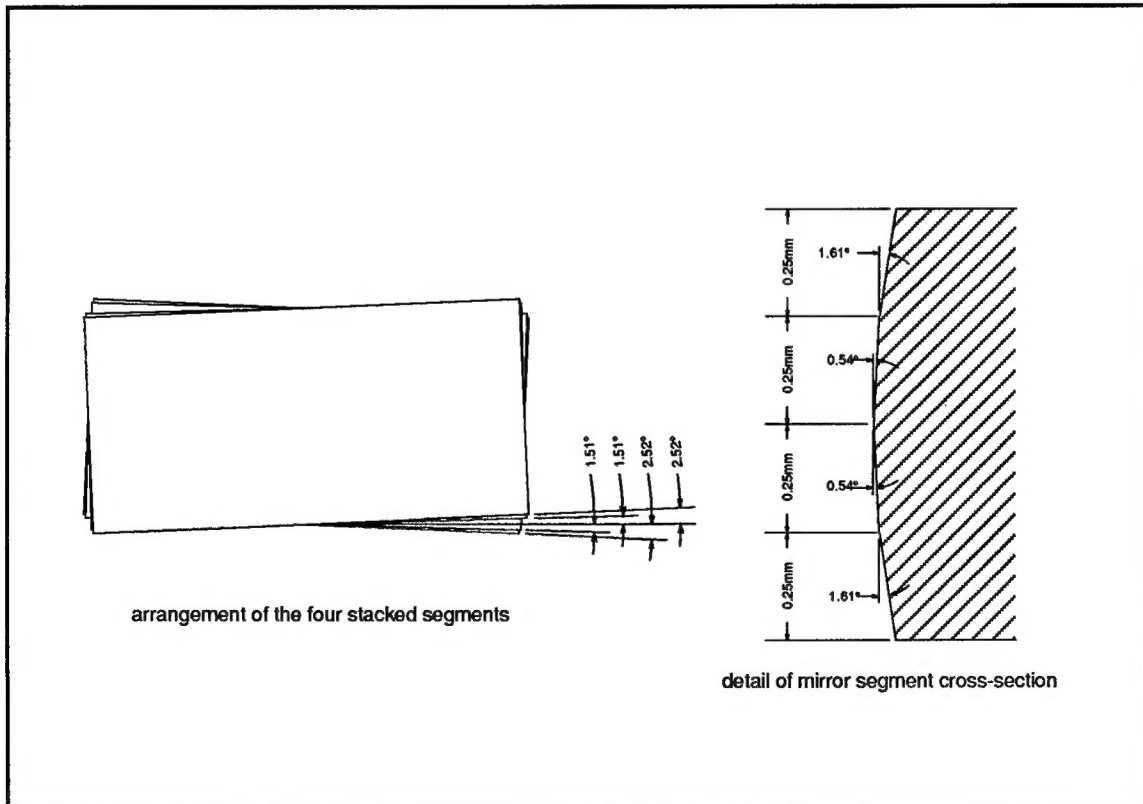


Figure 4: Spatial multiplex mirror array.

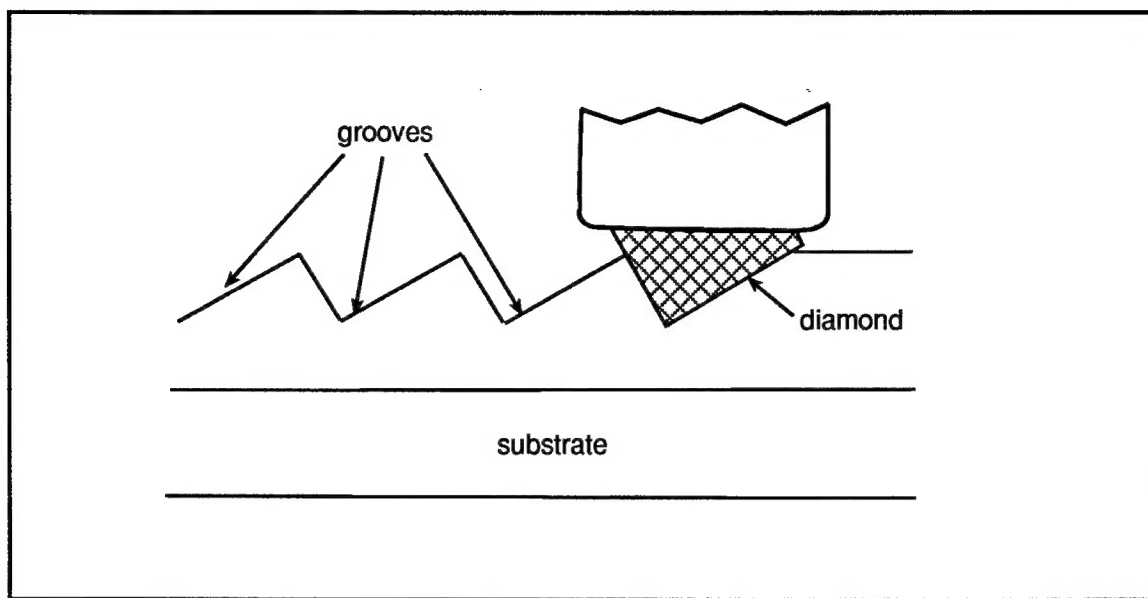


Figure 5: Fabrication of a blazed grating.

2.4 The Reference Beam. The reference beam scan generator is illustrated in Figure 6. The scan generator consisted of two crossed TeO_2 acousto-optic Bragg cells and a combination of cylindrical and spherical lenses that re-imaged the vertical and horizontal scan planes to a common plane, which then became the apparent scan source. Anamorphic optics were used in order to fill the rectangular 14 x 4 mm aperture of the Bragg cells, in order to produce the maximum number of resolvable spots in the scanned beam.

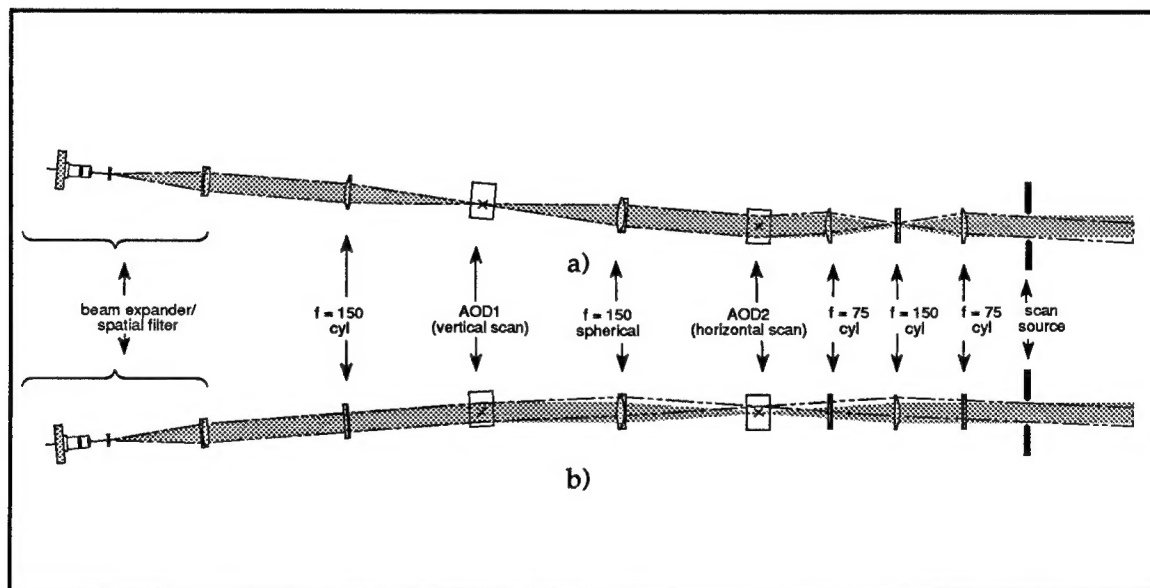


Figure 6: Reference beam scan generator with anamorphic optics; a) top view showing horizontal scan; b) side view showing vertical scan.

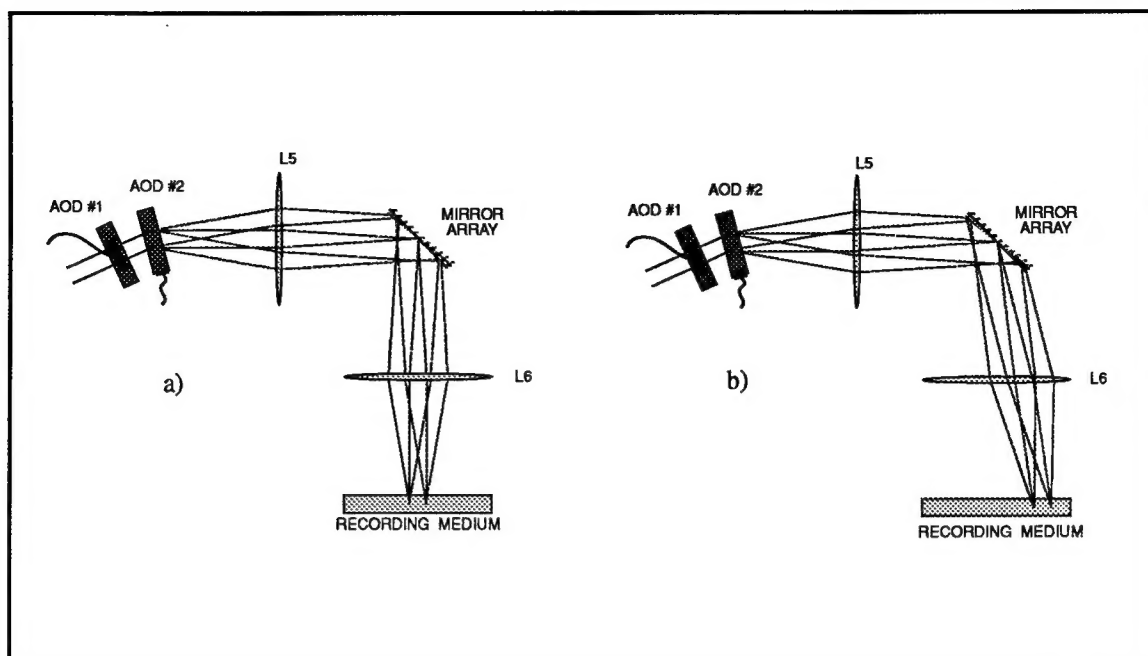


Figure 7: Reference beam angular and spatial multiplexing.

The Bragg cells, or AODs, had a center frequency of 80 MHz, a bandwidth of 50 MHz, and 1,100 resolvable spots. Each Bragg cell provided a total beam deflection of approximately 2° . Since the Bragg cells introduce Doppler frequency shifts, which in turn can cause the interference pattern to be recorded to drift, an electro-optic phase modulator was used (item 1 in Figure 1) to compensate for the unwanted frequency shifts. The two RF signals used to drive the Bragg cells were mixed and amplified to produce the drive signal for the phase modulator.

The reference beam scan generator and faceted mirror array worked together as shown in Figure 7. The scan generator produced an apparent scan source placed one focal length away from lens L5. This lens focused the beam onto the mirror array. Lens L6 recollimated the beam. As the beam was scanned horizontally by AOD2, the focused spot traveled along one mirror facet, thus changing the incidence angle at the crystal. This procedure provided angular multiplexing at each storage location. Lens L6 was one focal length away from the mirror array and the crystal, which kept the scanned beam stationary at the storage location. The focal length ratio of the two lenses determined the magnification of the scan angle. Here, the scan angle was magnified from approximately $\pm 1^\circ$ to $\pm 3^\circ$.

2.5 The Object Beam. The object beam architecture is shown in Figure 8. The object beam was deflected using manually scanned mirror M1. Lenses L1 and L2, together with lenslet array LA1, expanded the beam and magnified the scan angle. The scan mirror was one focal length away from L1, which directed the beam to one of 16 lenslets in LA1. L2 was one focal length away from both LA1 and the SLM. L2 recollimated the beam and directed it through the SLM. Lens L3 produced the Fourier transform of the SLM and directed it to one of 16 lenslets in LA2. LA2 projected the image of the SLM into the various storage locations in the crystals. LA3 took the reconstructed hologram images and multiplexed them onto the CCD. This object beam design was entirely telecentric, i.e., the

chief ray of each focused bundle is parallel to the optical axis. This ensured that there was no vignetting for the various scan positions.

2.6 Storage and Reconstruction. Referring to Figure 2, data holograms were stored within the Fe:LiNbO₃ crystals using the following procedure:

- (1) The crystals were cleaned and loaded into the crystal mounting fixture. The reference and object beams were blocked.
- (2) The object beam was manually directed to storage location 1 (of 16) by turning mirror M1.
- (3) The hologram recording procedure was then controlled via a Basic program on a 386 computer. The program prompted the user to input the number of storage locations to be used, the number of holograms to be stored at each location, the number of the first SLM image to be used and the total number of SLM images. (The exposure time for each hologram and the time delay before recording were both preset in the program.)
- (4) AOD1 (the vertical scan) and AOD2 (the horizontal scan) directed the reference beam to storage location 1 (of 16) and to recording angle 1 (of 100).
- (5) The Panasonic Optical Disk Drive, where the data-pages were stored, brought up the first page and direct it to the SLM. Each data-page was represented by a 24 by 40 checkerboard of randomly generated 1's and 0's, each checkerboard element consisting of an 8 x 10 array of SLM pixels.
- (6) The main shutter opened, the user was prompted to check that all beam paths were clear and that the correct image had been loaded into the SLM, and then the shutter was closed.
- (7) The time delay countdown was then initiated. The beam blocks were removed, the table enclosures closed and the room evacuated.

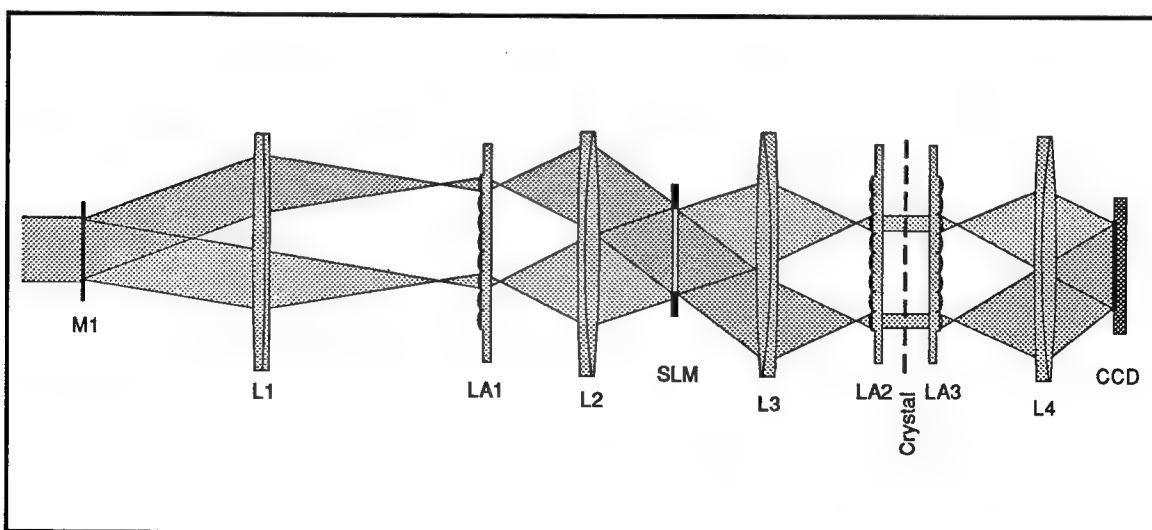


Figure 8: Object beam spatial multiplexer schematic.

- (8) After the countdown was completed, the main shutter opened for a predetermined time to expose the first hologram (30 seconds in this case).
- (9) AOD2 then incremented the reference beam incidence angle, and the SLM incremented to the next data-page image.
- (10) The main shutter opened to expose the next hologram.
- (11) Steps 9 and 10 were repeated until all holograms were recorded at that storage location (100 holograms in this case).
- (12) The program then prompted the user to direct the object beam to the next storage location and waited for a response. The user then blocked the object and reference beams, opened the main shutter, manually turned M1 (sending the object beam to the next storage location), and closed the shutter.
- (13) Steps 7 through 12 were then repeated until all holograms were recorded (1,600 in this case).
- (14) Once all of the holograms had been recorded, readout was done by blocking the object beam and scanning the reference beam through all of the recording angles. The reconstructed object beam was imaged onto the CCD, which was connected to a VCR.
- (15) Finally, the holograms were erased by baking the crystals at 240°C for several hours.

2.7 Design Modifications. As noted in the Introduction, the actual object beam architecture used represented a modification of the proposed configuration. The object beam was originally designed to be scanned using acousto-optic Bragg cells. This design was modified, however, when interferometric tests revealed frequency jitter problems with the radio-frequency (RF) sources driving the object beam Bragg cells. (The reference beam RF sources did not exhibit this problem.) The defective components (Isomet model LS110-500) were replaced with a manually scanned mirror. Also, the proposed configuration was designed to record Fourier-space holograms, i.e., the Fourier plane of the SLM was placed at the crystals. The actual architecture recorded image-space holograms, i.e., the SLM was re-imaged at the crystals. This change was made because recording Fourier holograms necessitated placement of a random phase encoder immediately adjacent to the SLM in order to efficiently utilize the entire recording volume. An appropriate phase encoder was not available at the time the system was built. Changing to image-space holograms involved the addition of two lenslet arrays, one on either side of the crystals (LA2 and LA3 of Figure 8).

Other minor changes were made in the reference arm of the memory. Significant path length was added to the reference beam in order to equalize the path lengths of the object and reference beams and, thereby, keep their path length difference well within the coherence length of the argon laser. Spherical optics in the scanner portion were also replaced with cylindrical optics in order to utilize the full aperture of the Bragg cells. Finally, the beam path near the crystal was changed so that the reference and object beams were incident on the same side of the crystal (with an interbeam angle of 60°) in order to record transmission holograms. The latter was found to be the optimum figure-of-merit

configuration. The proposed architecture had the reference and object beams incident on opposite sides of the crystal in order to record reflection holograms.

3.0 Results

3.1 Storage and Reconstruction Results. We successfully recorded 1600 holograms containing 1.5 megabits of data with the HRAM system. 100 holograms were recorded at each of 16 locations in 4 crystals, each hologram containing 960 bits of data. The conceptual design for angular and spatial multiplexing utilizing a non-mechanically scanned reference beam was also successfully demonstrated. The holograms did, however, exhibit obvious problems that can be corrected using the appropriate design modifications.

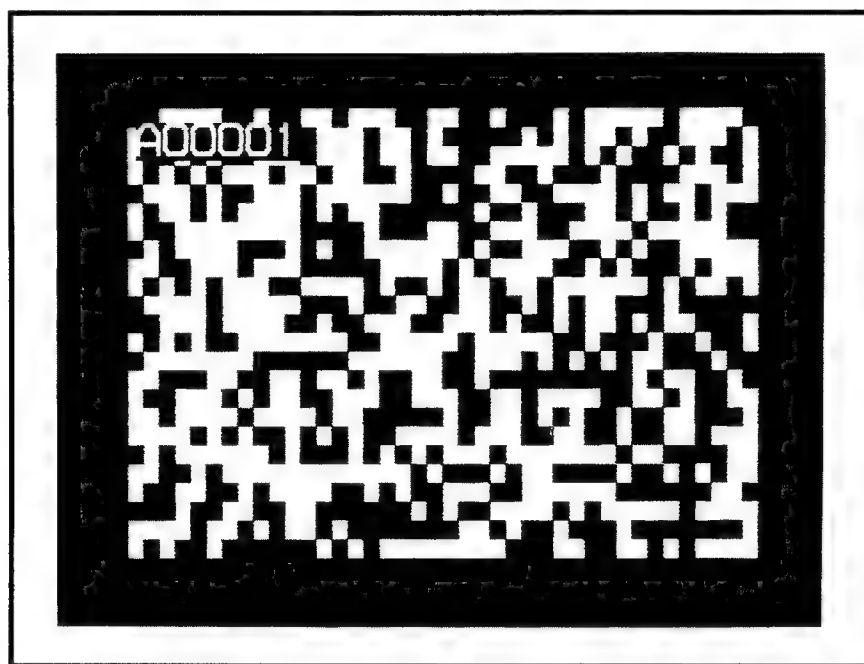


Figure 9: Input data-page image.

The reference beam of the HRAM was completely non-mechanically scanned. The mirror array and Bragg cells functioned together as designed to provide for both angular and spatial multiplexing. The frequency shift compensation provided by the E-O phase modulator kept the object and reference beams coherent with one another to provide good fringe contrast at the crystals. As noted in the Architecture section, the object beam was not non-mechanically scanned as originally proposed, although the concept of non-mechanical scan demonstrated with the reference arm could be easily implemented in the object beam using properly functioning equipment.

Figure 9 shows one of the input images that was loaded into the SLM. Prior to storing 1,600 holograms, a test run was performed by recording 10 holograms at one location. Figure 10 shows a reconstructed image from this run.

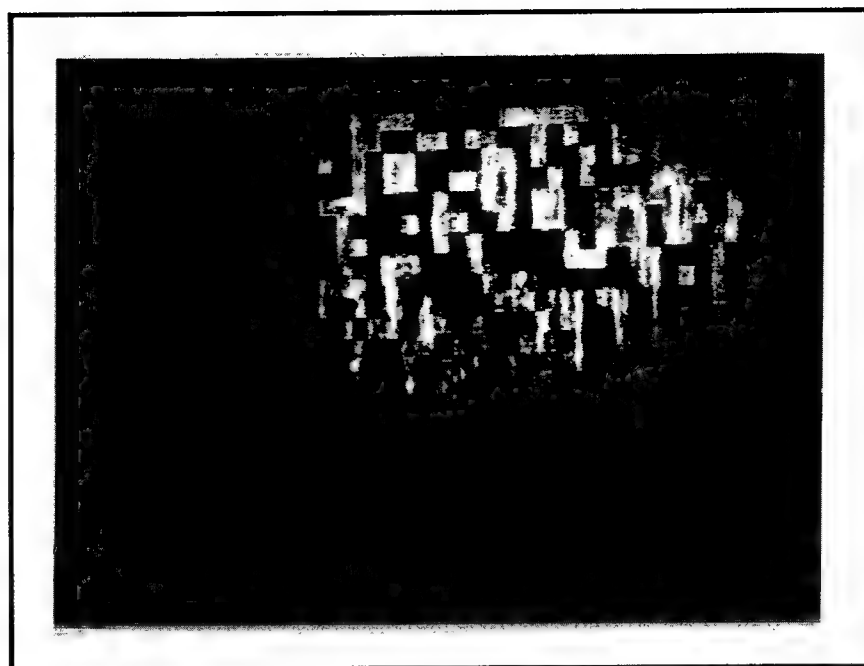


Figure 10: Reconstructed image, 1 of 10.

Results of the 1,600 hologram run are shown in Figures 11a and b. The imperfections in these images indicate design issues that are well understood at present and correctable in future designs. The images exhibit non-uniform intensity, crosstalk, vertical striations and brightness variations from hologram to hologram.

3.2 Hologram Non-Uniformity. The non-uniform intensity is attributable mainly to imperfections in the mirror array. The mirror array distorted the reference beam and smeared the energy vertically, causing non-uniform illumination during both recording and reconstruction. The result was multiplicative noise on the reconstructed hologram. The mirror array was fabricated in the same manner as ruled diffraction gratings. This process tends to leave grooves and sleeks along each mirror facet, which in turn causes beam spreading perpendicular to the grooves. This problem can be corrected by polishing each facet. Figure 12 shows a false-color display of the reference beam intensity.

Object beam intensity fall-off (from the center of the SLM to its edges) also contributed to the non-uniform appearance of the reconstructed holograms. Ideally, a more powerful object beam could be expanded sufficiently to overcome this problem.

3.3 Crosstalk. Correlation crosstalk was also apparent, especially among the first 100 holograms of a short, high-efficiency sequence. Correlation crosstalk occurs when spatially non-orthogonal holograms are recorded using an architecture (like the HRAM) in which the object beam remains fixed in direction. In such an architecture, the storage of a data-page generates partial reconstruction of all previously used reference beams whose associated data-pages are not orthogonal with the current data-page. These reconstructions (whose individual strengths are proportional to the vector projections of the current data-page onto each previously recorded data-page) interfere with the current reference beam to form "bridging" plane-wave holograms, which then couple (to some extent) all holograms together. This effect may be mitigated (although never completely eliminated) by

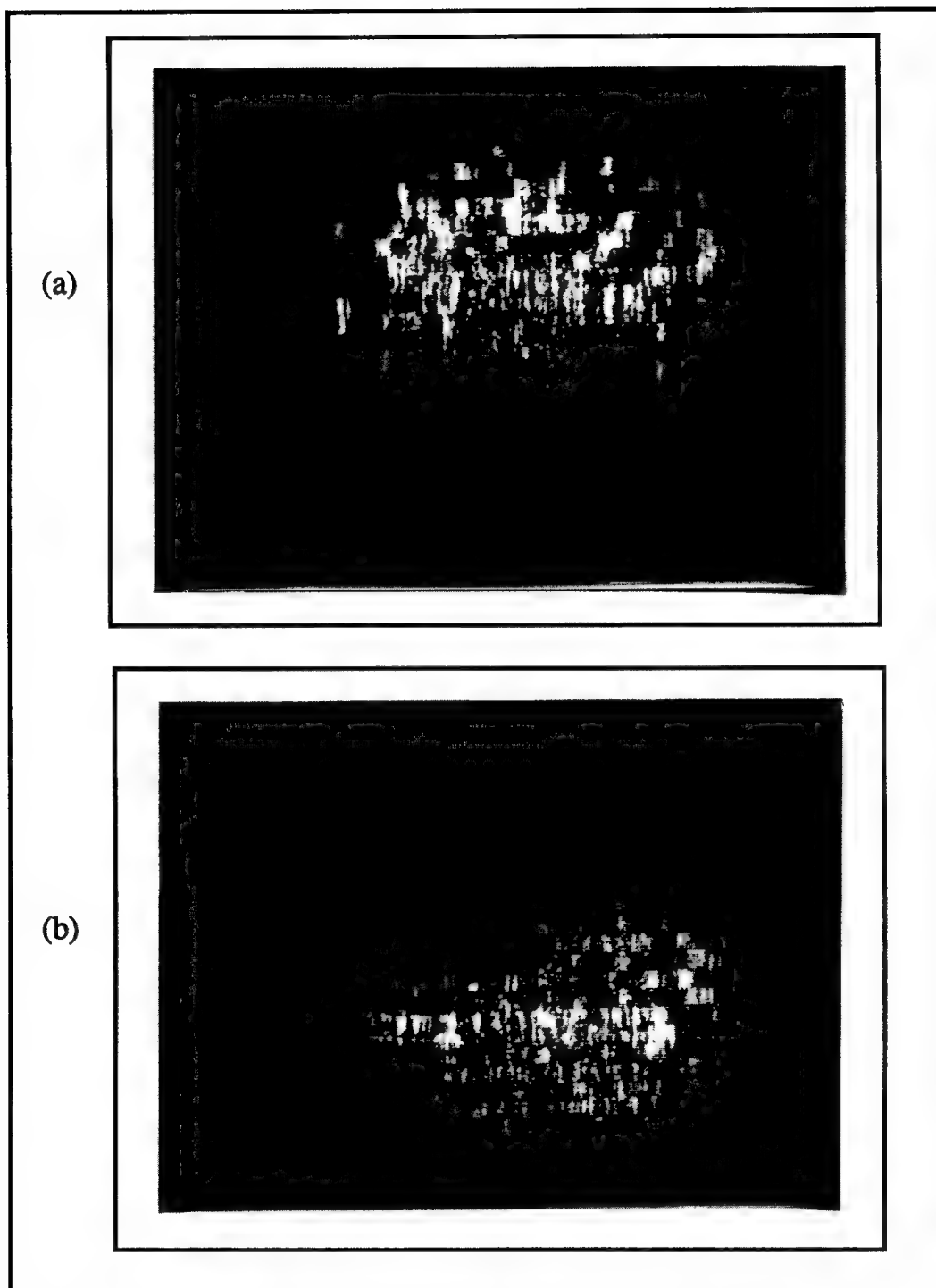


Figure 11: Reconstructed images, a) first of 100 holograms, and b) last of 100 holograms.

modifying the hologram storage schedule in such a way that high-efficiency holograms are not recorded sequentially. A subsequent enhancement or refreshing step (see, for example, references [7] and [8]) can then be used to bring all holograms up to their maximum values.

3.4 Photorefractive Damage. Vertical striations in the holograms indicate photorefractive damage. In the present configuration, we recorded image-space holograms. In this arrangement, each storage location in the crystals was repeatedly exposed to the pixel grid pattern of the SLM, which then became "burned" into the crystal. This damage could be observed visually by inspecting the crystals after recording (and could be removed by baking out the crystal). This problem can be avoided by recording Fourier-space holograms. To implement this, the lenslet arrays on either side of the crystals could be removed, and a customized random phase encoder inserted adjacent to the SLM.

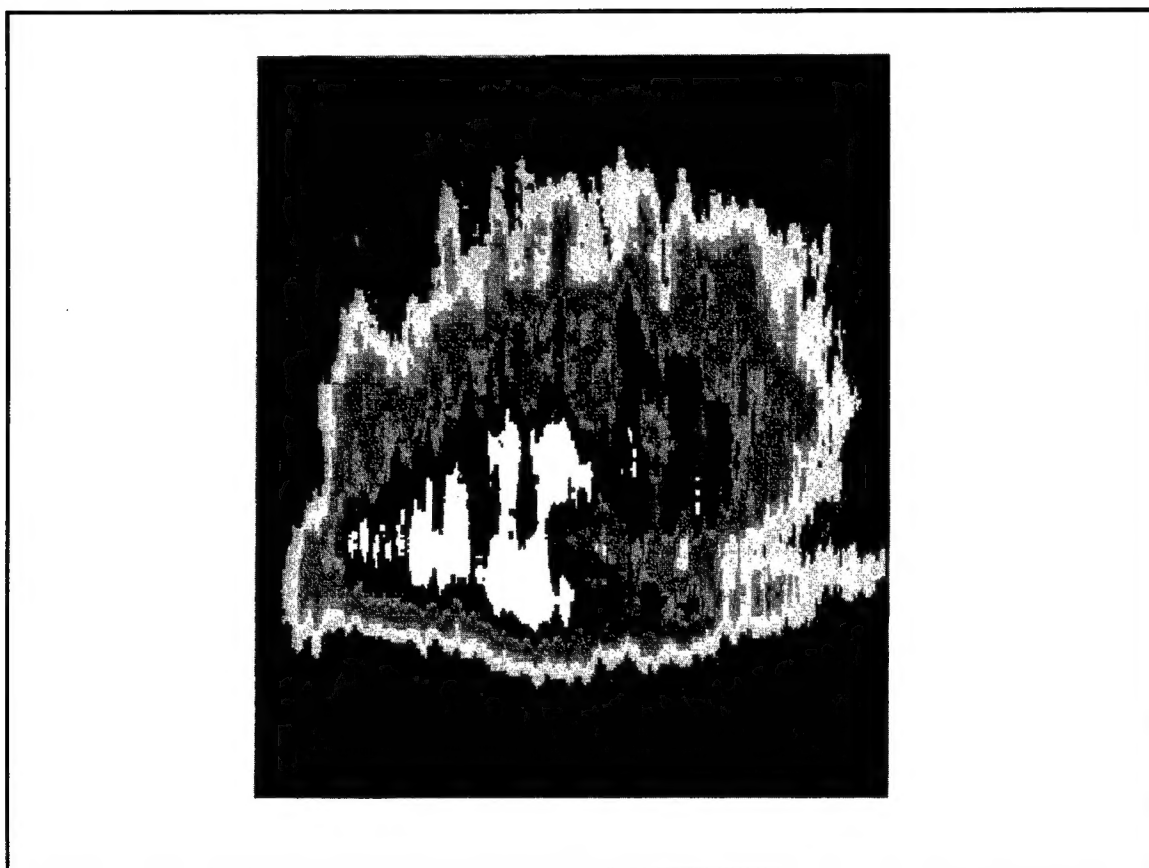


Figure 12: Reference beam intensity profile after mirror array.

3.5 Vibrations. The holograms also required fairly long exposures (30 seconds to 1 minute per hologram). Such long exposures made them extremely susceptible to vibrations and air currents, thereby resulting in significant variations in diffraction efficiency from hologram to hologram. Providing more energy at the crystals by using a higher power laser and reducing optical losses would allow shorter exposure times. A more complicated alternative solution would involve some form of active path-length compensation.

4.0 Conclusions

The results obtained by Northrop and California Institute of Technology demonstrated, at least qualitatively, that fast ($< 10 \mu\text{sec}$), non-mechanical addressing techniques could, in principle, be used to randomly access large numbers ($\sim 10^4$) of angle-multiplexed holograms stored within separate regions of Fe:LiNbO_3 . Much additional work must, however, be done to prove that 3-D holographic memories are (1) technically feasible, and (2) economically viable.

Recent and rapid advances in the development of several key memory components, however, suggest that many of the toughest technical issues may soon be resolved. Solid-state, blue/green lasers (frequency-doubled Nd:YAG and Nd:YLF) capable of more than 0.5 W average power output will, for example, soon be commercially available. Likewise, as a result of commercial efforts to develop high-resolution, head-mounted displays and low-cost, high-definition television, megapixel, gray-scale SLMs capable of 30 Hz frame rates are also on the horizon, with megapixel, binary, kHz frame rate SLMs nearing a similar level of maturity. Finally, highly uniform, megapixel CCD arrays with very low read noise and large dynamic range are already available from a number of manufacturers.

More difficult are the economic issues which must be confronted. These include the lack of basic manufacturing infrastructures (i.e., facilities required to manufacture the laser, the electro-optic and acousto-optic modulators, and the SLM, and those required to grow large quantities of Fe:LiNbO_3) and a memory design point which can compete economically with projected, conventional memory types (mainly hard disks and tape libraries). Efforts should be focused on developing a niche market product which can support the capitalization necessary to "jump-start" the technology. Economics of scale can then be exploited to gradually increase production and, simultaneously, reduce product cost.

References

- [1] P.J. Van Heerden, *Appl. Optics*, **2**, 393 (1963).
- [2] J.J. Amodei and D.L. Staebler, *Appl. Phys. Lett.*, **20**(2), 79 (1972).
- [3] J.P. Huignard, F. Micheron, and E. Spitz, "Optical Systems and Photosensitive Materials for Information Storage", in *Optical Properties of Solids*, B.O. Seraphin, editor, Chapter 16, pages 847-925, North Holland, Amsterdam, 1976.
- [4] R.A. Bartonlini, A. Bloom, and J.S. Escher, *Appl. Phys. Lett.*, **28**, 506 (1976).
- [5] F.H. Mok, M.C. Tackitt, and H.M. Stoll, *Opt. Lett.*, **16**(8), 605 (1991).
- [6] F.H. Mok and H.M. Stoll, *Optical Pattern Recognition*, **1701**, 312 (1992).
- [7] D. Brady, K. Hsu, and D. Psaltis, *Opt. Lett.*, **15**(14), 817 (1990).
- [8] S. Piazzolla, B.K. Jenkins, and A.R. Tanguay, *Opt. Lett.*, **17**(9), 676 (1992).

MISSION
OF
ROME LABORATORY

Mission. The mission of Rome Laboratory is to advance the science and technologies of command, control, communications and intelligence and to transition them into systems to meet customer needs. To achieve this, Rome Lab:

- a. Conducts vigorous research, development and test programs in all applicable technologies;
- b. Transitions technology to current and future systems to improve operational capability, readiness, and supportability;
- c. Provides a full range of technical support to Air Force Materiel Command product centers and other Air Force organizations;
- d. Promotes transfer of technology to the private sector;
- e. Maintains leading edge technological expertise in the areas of surveillance, communications, command and control, intelligence, reliability science, electro-magnetic technology, photonics, signal processing, and computational science.

The thrust areas of technical competence include: Surveillance, Communications, Command and Control, Intelligence, Signal Processing, Computer Science and Technology, Electromagnetic Technology, Photonics and Reliability Sciences.